

RESEARCH ARTICLE | APRIL 28 2023

Density functional study of heteroatoms effect on corrosion inhibition efficiency of methenamine and its derivatives

Saprizal Hadisaputra ✉; Uci Ramadan; Made Ganesh Darmayanti



AIP Conference Proceedings 2619, 040006 (2023)

<https://doi.org/10.1063/5.0122519>



CrossMark

Articles You May Be Interested In

Photoresponse of sol-gel-synthesized ZnO nanorods

Appl. Phys. Lett. (May 2004)

Mangosteen peel extract as a green corrosion inhibitor of mild steel in 1 M hydrochloric acid: Gravimetric, quantum chemical, and Monte Carlo simulation studies

AIP Conference Proceedings (August 2022)

Individual heteroatom identification with X-ray spectroscopy

Appl. Phys. Lett. (April 2016)



Time to get excited.

Lock-in Amplifiers – from DC to 8.5 GHz



Find out more



Density Functional Study of Heteroatoms Effect on Corrosion Inhibition Efficiency of Methenamine and Its Derivatives

Saprizal Hadisaputra^{1, a)}, Uci Ramadan^{2, b)}, Made Ganesh Darmayanti^{2, c)}

¹Chemistry Education Division, University of Mataram. Jalan Majapahit No 62, Mataram, 83125, Indonesia

²Department of Chemistry, University of Mataram, Jalan Majapahit 62, Mataram, 83125, Indonesia

^{a)}Corresponding author: rizal@unram.ac.id

^{b)}uciramadan54@gmail.com

^{c)}ganesh@unram.ac.id

Abstract. A theoretical study on the corrosion inhibition performance of methenamine derivatives has been carried out using density functional theory. Experimental studies have been carried out previously using gravimetry and electrochemical impedance spectroscopy on the corrosion inhibition efficiency of methenamine against carbon steel. However, the study of the effect of heteroatom changes (nitrogen, phosphorus, and boron) on the efficiency of corrosion inhibition of methenamine derivatives has not been studied in more detail. Corrosion inhibition efficiency is based on the value of quantum parameters, namely high occupied molecular orbital, low unoccupied molecular orbital, energy gap, ionization potential, electronegativity, and the number of electron transfers. The addition of two boron atoms shows that it has the highest corrosion inhibition efficiency. It is described in detail using the values of the quantum parameters. Fukui function and second-order interaction energy determine the active site and corrosion inhibition strength. This theoretical study is expected to assist in designing efficient and environmentally friendly corrosion inhibitors.

INTRODUCTION

Corrosion is a process that destroys the metal structure due to its interaction with a corrosive environment. Corrosion will cause large economic losses if the corrosion process is allowed without prevention [1,2]. Therefore, research to find anti-corrosion materials that are easy to use, economical, and high efficiency is still being intensively carried out. One corrosion inhibitor that is continuously being researched is a corrosion inhibitor based on organic compounds. The selection of organic molecules as corrosion inhibitors is environmentally friendly, non-toxic, and does not cause harmful pollutants [3-5]. Various types of organic compounds have been used as anti-corrosion compounds. The efficiency of corrosion inhibition of organic molecules is determined by the heteroatom groups (O, N, S, and P) and bond contributions from the double or triple bonds. The presence of suitable functional groups will help the formation of complexes between organic compounds and metal surfaces by coordinating covalent bonds (chemical adsorption) or electrostatically (physical adsorption) [5-7]. Organic molecules will regularly adhere to the metal surface to form a uniform layer that can prevent the metal surface from coming into contact with corrosive media [8-10].

Many studies on corrosion inhibition of organic molecules have been carried out experimentally and theoretically [11-16]. Several synthetic organic molecules' adsorption and corrosion inhibitory performance against mild steel experimentally and theoretically. Experimental studies can prove that corrosion protection occurs on the surface of mild steel by forming an organic film. Density functional theory and molecular dynamics were used to

study the mechanism of inhibition on mild steel surfaces. Organic molecules adhere parallel to the mild steel surface, which indicates that the corrosion inhibition process runs optimally [17]. In addition to synthetic molecules, natural products have also been widely used as corrosion inhibitors [17-22]. The inhibition of corrosion by thevetia peruviana flower extracts experimentally and theoretically has been studied. Experimental studies showed good corrosion inhibition efficiency by following the Temkin Adsorption isotherm. Molecular modeling was carried out to strengthen experimental studies. It shows an interaction between electron donor and acceptor of organic and metal molecules. The orientation of organic molecules can also be described clearly, forming a flat on the metal surface [23].

Methenamine compound is one of the potential organic inhibitor compounds. It has four tertiary nitrogen atoms and has a tricyclo geometric structure. The four N atoms have the potential to interact with metal surfaces to protect metals from corrosion processes [24-25]. Studies on the inhibitory power of methenamine have been previously reported using the potentiodynamic polarization (Tafel) and electrochemical impedance spectroscopy (EIS) measurement methods [26]. Potentiodynamic and EIS measurements, the maximum inhibition efficiency value obtained was 71.55% using the Tafel method, while the EIS method was obtained at 70.21% for a 100 ppm methenamine concentration. In general, the value of inhibition efficiency increased with the increasing concentration of inhibitors added to the test medium. So far, however, studies on the effect of heteroatoms on methenamine as a corrosion inhibitor have not been published. This research focuses on testing the effect of heteroatom changes (nitrogen, phosphorus, and boron) on the efficiency of the corrosion inhibitors derived from methenamine.

RESEARCH METHODOLOGY

Density functional theory was applied with the B3LYP hybrid function. The base sets used for the methenamine molecule are 6311++G(d,p) and LANL2DZ ECP for metals. The optimization of the molecular geometry of the inhibitor was carried out using gaussian 09 [27]. Energy calculations were carried out to determine the efficiency of the inhibitor in the gas phase and the solution phase. Then calculate the interaction energy, Mulliken atomic charge (Fukui), and Natural Bond Orbital (NBO). The determination of quantum parameters such as high occupied molecular orbital EHOMO, low unoccupied molecular orbital ELUMO, ionization potential (I), electronegativity (χ), and the number of electron transfers (ΔN) [28-34] is generated from the following equation.

$$I = -E_{\text{HOMO}} \quad (1)$$

$$A = -E_{\text{LUMO}} \quad (2)$$

$$\chi = \frac{I + A}{2} \quad (3)$$

$$\eta = \frac{I - A}{2} \quad (4)$$

$$\Delta N = \frac{\chi_{\text{Fe}} - \chi_{\text{Inh}}}{2(\eta_{\text{Fe}} + \eta_{\text{Inh}})\pi r^2} \quad (5)$$

The correlation of the quantum chemical parameters with the corrosion inhibitor performance has been determined using equation 6-8 [35,36]:

$$I_{\text{add}}\% = \frac{I_{\text{Inh}} - I_{\text{X-Inh}}}{I_{\text{Inh}}} \times 100\% \quad (6)$$

$$IE_{\text{add}}\% = I_{\text{add}}\% - I_{\text{eInh}}\% \quad (7)$$

$$IE_{\text{theor}}\% = I_{\text{eInh}}\% + IE_{\text{add}}\% \quad (8)$$

$I_{\text{add}}\%$ is the percentage ionization potential, $IE_{\text{add}}\%$ is the inhibition efficiency %, and $IE_{\text{theor}}\%$ is the theoretically calculated percentage inhibition efficiency.

The magnitude of the interaction energy value (ΔE) is closely related to the stability of the complex formed. The stable complex has a low interaction energy (ΔE). So the more negative E , the more stable the complex formed. The interaction energy (ΔE) is obtained from the difference between the energy of the complex ($\Delta E_{\text{Complex}}$) with the energy of the ligand (ΔE_{Ligand}) and the energy of iron (ΔE_{Fe}) in equation 9.

$$\Delta E = \Delta E_{\text{Complex}} - (\Delta E_{\text{Ligand}} + \Delta E_{\text{Fe}}) \quad (9)$$

Natural Bond Orbital used the second population analysis, namely E2. E2 represents the intensity of each electron donor between Lewis Donors (i) and non-Lewis NBO Acceptors (j). E2 with respect to $i \rightarrow j$ delocalization is estimated as follows:

$$E2 = q_i \frac{F(i,j)}{\epsilon_i - \epsilon_j} \quad (10)$$

Here, q_i is the occupancy of the donor orbital. whereas i, j are diagonal elements (orbital energy), and $F(i, j)$ are off-diagonal elements [37,38].

Fukui analysis is defined:

$$f = \left(\frac{\partial p(\vec{r})}{\partial N} \right)_{v(\vec{r})} \quad (11)$$

Fukui can be measured for nucleophilic attack as follows [39]:

$$f^+ = q(N+1) - QN \quad (12)$$

while the electrophilic attack:

$$f^- = QN - q(N-1) \quad (13)$$

q is the total charge of the inhibitor atom, $q(N+1)$ is the charge of the cation, QN is the charge of the neutral molecule, and $q(N-1)$ is the charge of the anionic form.

RESULT AND DISCUSSION

The optimization of the methenamine molecule with the selected theoretical level can be seen in Figure 1. The optimized structure will provide information about the molecular geometry in bond distances and bond angles. Bond angle affects the distribution of electrons in a molecule and the molecule's flexibility. The bond angle is the angle formed by the central atom at the top with two atoms around it. The larger the angle formed by the atoms, the less flexible the formed molecule. Methenamine has a low degree of flexibility which allows methenamine to be used as a corrosion inhibitor. Table 1 shows the comparison results between the tie distance and the tie angle with the average difference, namely the tie distance of 0.022, while the tie angle is 0.995° . Table 1 shows the suitability of the structural parameters from theoretical to experimental [40] so that the selected theoretical level has high accuracy. It also shows that the theoretical level used can be applied to the studied system.

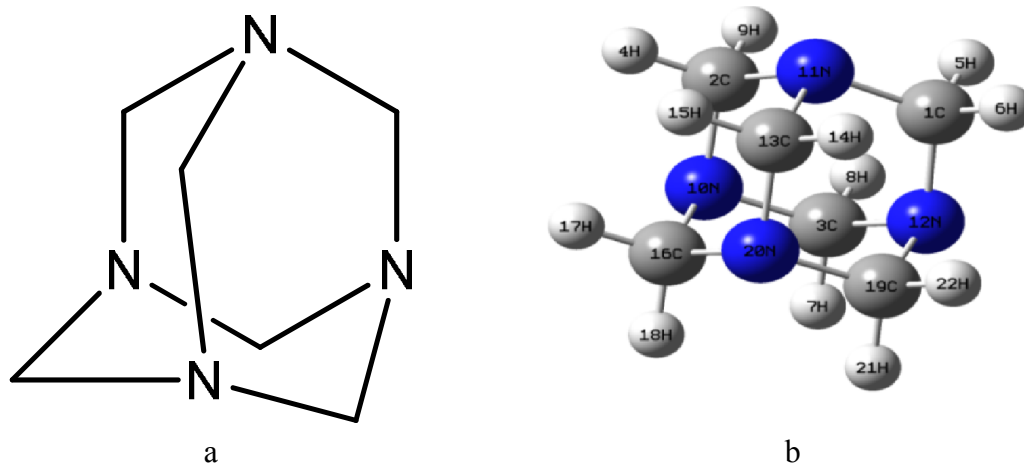


FIGURE 1. The 2D and 3D of methenamine structures.

TABLE 1. Comparison of bond length (Å) and bond angle from theoretical calculations at the level of DFT/B3LYP/6-311++G(d,p)

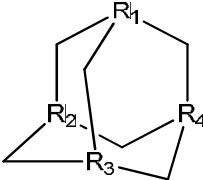
Bond Length	Exp* (Å)	Theory (Å)	Bond Angle	Exp* (°)	Theory (°)
C1-N12	1.47597	1.47627	C1-N12-C19	108.850	107.765
N12-C19	1.47601	1.47647	N12-C19-N20	111.887	112.773
C19-N20	1.52864	1.47645	C19-N20-C16	106.801	107.756
N20-C16	1.52876	1.47641	N20-C16-N10	111.897	107.781
C16-N10	1.45374	1.47633	C16-N10-C2	108.833	112.770
N10-C2	1.47596	1.47635	N10-C2-N11	112.088	107.766
C2-N11	1.47626	1.47620	C2-N11-C1	108.239	112.795
N11-C1	1.47621	1.47642	N11-C1-N12	112.068	107.765
N11-C13	1.45381	1.47631	N11-C13-N20	111.894	112.764
C13-N20	1.52870	1.47639	N12-C3-N10	112.088	112.779

Quantum parameters function as a determination of structural properties so that they can be used to predict which compounds are more efficient as corrosion inhibitors. The HOMO energy indicates the nature of the molecule to donate its electrons. The smaller the energy difference between HOMO-LUMO, the compound's electrons are more easily excited to a higher energy level so that the compound is more reactive [41-45]. HOMO energy is one factor that affects the reactivity of a molecule. If the HOMO energy is high, then the ionization energy is smaller, making it easier to transfer electrons for chemical bonds to occur. Table 2 shows the increase in the EHOMO value of methenamine and its heteroatomic groups in the following order MB4 > MN4 > MNB3 > MN3P > MP4 > MN3B > MN2P2 > MNP3 > MN2B2 in the solution phase. Based on these data, it can be predicted that the addition of 2 boron atoms to methenamine has a higher corrosion inhibition efficiency than other compounds. The LUMO energy (ELUMO) indicates the nature of the molecule to accept electrons. The larger the EHOMO or the smaller the ELUMO, the stronger an organic molecule to attach to metal cations so that the organic molecule will have high anti-corrosion efficiency [46,47]. Table 2 shows the ELUMO values from the largest to the smallest, namely MB4 > MNB3 > MN2B2 > MN3B > MP4 > MNP3 > MN2P2 > MN3P > MN4 in the solution phase. It shows that MB4 has the lowest inhibition efficiency.

The energy gap can determine the reactivity of a compound. The reactivity of the compound is related to the value of the efficiency of inhibition. The more reactive a compound is, the easier it can bind to metals and increase inhibition efficiency. The small energy gap indicates the energy of electron transfer from HOMO to LUMO is small, thus enabling electron transfer or electron excitation easily [48,49]. Table 2 shows that the Egap energy gaps are MN4 > MN3P > MP4 > MN2P2 > MNP3 > MN3B > MNB3 > MB4 > MN2B2. Molecules with low energy gaps are generally associated with high chemical reactivity and low molecular stability. Methenamine has a large energy gap value of -5.896 eV in the gas phase and -6.127 eV in the water phase so that it tends to be stable, so its reactivity is less in metals.

The ionization potential (I) can measure the reactivity of atoms or molecules. A high ionization potential value indicates a molecule has high reactivity, while a low ionization potential value indicates low reactivity. A low ionization potential value indicates a molecule has high reactivity, while a high ionization potential value indicates low reactivity [29, 50, 51]. Table 2 shows that the potential energy from the addition of 2 Boron atoms is the lowest at 5.225 eV in the gas and solution phases, while the addition of 4 Boron atoms is the lowest from the addition of other atoms. The addition of 2 Boron atoms has low reactivity and has a higher anti-corrosion efficiency which is correlated with the value of $r^2 = 0.98942$ (Figure 2).

TABLE 2. Parameters of Quantum Descriptor DFT B3LYP 6-311++G (d,p)



R1 = N, B, P
R2 = N, B, P
R3 = N, B, P
R4 = N, B, P

Gas Phase									
Parameter	MN4	MN3B	MN2B2	MNB3	MB4	MN3P	MN2P2	MNP3	MP4
E _{HOMO} (eV)	-6.246	-5.670	-5.225	-6.041	-7.444	-5.852	-5.555	-5.405	-5.847
E _{LUMO} (eV)	-0.350	-1.103	-1.548	-1.609	-3.328	-0.352	-0.388	-0.443	-0.496
E _{gap} (eV)	5.896	4.566	3.677	4.432	4.115	5.499	5.167	4.961	5.350
I (eV)	6.246	5.670	5.225	6.041	7.444	5.852	5.555	5.405	5.847
A (eV)	0.350	1.103	1.548	1.609	3.328	0.352	0.388	0.443	0.496
χ (eV)	3.298	3.387	3.387	3.825	5.386	3.102	2.971	2.924	3.172
ΔN	0.627	0.791	0.982	0.716	0.391	0.708	0.779	0.821	0.715
IE _{theor} %	70.21	76.69	81.68	72.52	56.74	74.64	77.98	79.66	74.70
Aqueous Phase									
E _{HOMO} (eV)	-6.368	-5.768	-5.294	-6.008	-7.403	-5.908	-5.560	-5.377	-5.870
E _{LUMO} (eV)	-0.240	-1.011	-1.536	-1.620	-3.280	-0.224	-0.243	-0.272	-0.340
E _{gap} (eV)	6.127	4.756	3.757	4.388	4.123	5.683	5.316	5.105	5.530
I (eV)	6.368	5.768	5.294	6.008	7.403	5.908	5.560	5.377	5.870
A (eV)	0.240	1.011	1.536	1.620	3.280	0.224	0.243	0.272	0.340
χ (eV)	3.304	3.389	3.415	3.814	5.341	3.066	2.901	2.824	3.105
ΔN	0.603	0.759	0.953	0.725	0.402	0.692	0.770	0.817	0.704
IE _{theor} %	70.21	76.83	82.05	74.17	58.80	75.28	79.12	81.13	75.69

Table 2 shows that the electron affinities are MB4 > MNB3 > MN2B2 > MN3B > MP4 > MNP3 > MN2P2 > MN3P > MN4. It shows that MB4 is predicted to have poor inhibition efficiency. It is also found in the electronegativity parameter. The addition of 4 Boron atoms has a high electronegativity value among other atoms, which is 5.386 eV. The electronegativity value for the addition of 2 Boron atoms is 3.387 eV in the gas phase, as is the case with the solution phase. The addition of 2 boron has good anti-corrosion properties compared to other atoms, while four boron atoms have poor corrosion efficiency.

The highest electron transfer will produce the best inhibitor efficiency. The largest number of electron transfers is the addition of 2 Boron atoms MN2B2 in the solution phase of 0.953 eV. The smallest electron transfer value is obtained in compounds with the addition of 4 Boron atoms, which is 0.391 eV. It predicts that MN2B2 has the highest corrosion inhibition efficiency and MB4 vice versa. Figure 2 shows the positive correlation between the transferred electrons. Positive correlation between transferred electrons and corrosion inhibition efficiency with a correlation value of $r^2 = 0.92665$. The addition of 4 Boron atoms showed a less good corrosion inhibitor than phosphorus atoms. MN2B2 has the highest electron transferability, while methenamine compounds show the lowest electron transferability.

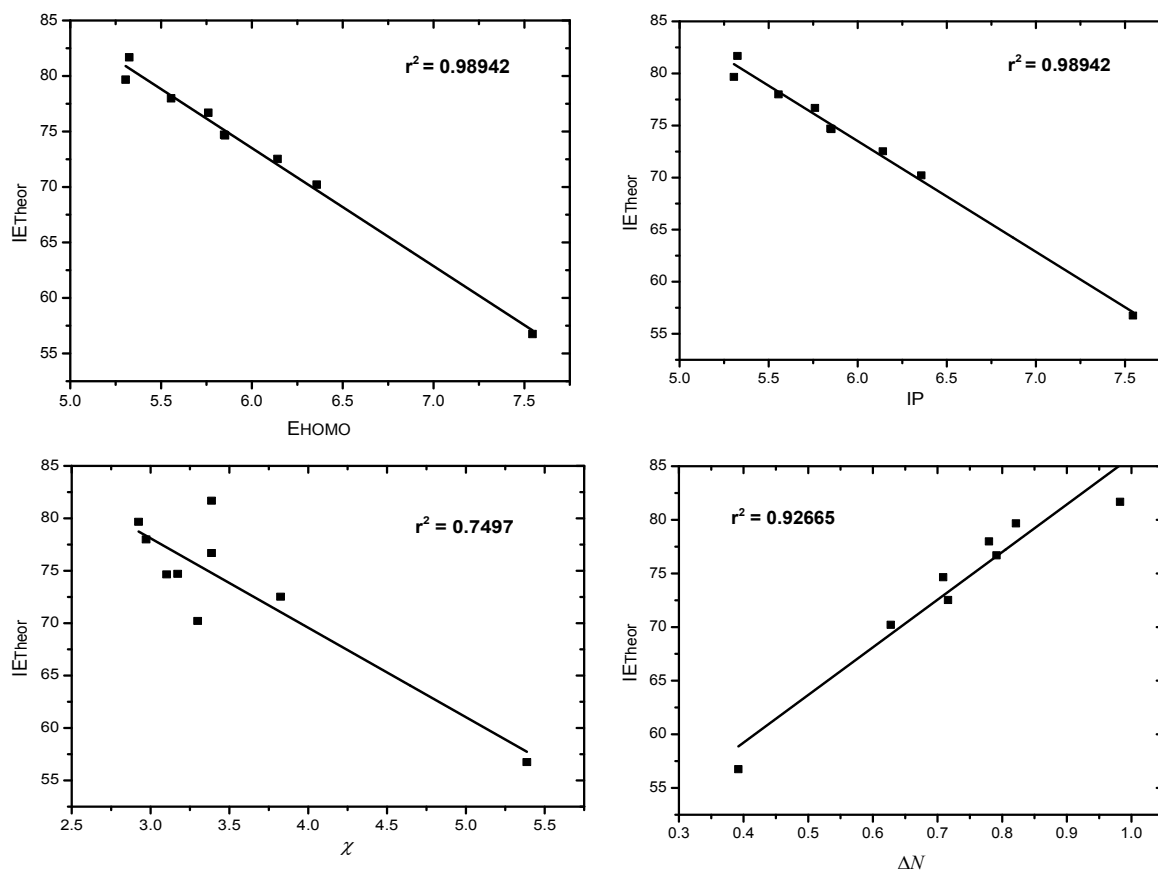


FIGURE 2. The relationship between quantum parameters and corrosion inhibition efficiency measured by the DFT/6-311++G method (d,p)

TABLE 3. The theoretical percentage of inhibition efficiency (IEtheor.%)

Inhibitors	ΔE . kcal.mol ⁻¹	IETheor. %	
		Gas	Aqueous
MN4	-36.7766	70.21	70.21
MN3B	-40.4251	76.69	76.83
MN2B2	-40.9306	81.68	82.05
MNB3	-41.2853	72.52	74.17
MB4	-41.5521	56.74	58.80
MN3P	-21.2455	74.64	75.28
MN2P2	-41.9940	77.98	79.12
MNP3	-45.2962	79.66	81.13
MP4	-57.7755	74.70	75.69

Table 3 shows the results of theoretical calculations on corrosion inhibition efficiency. The theoretical efficiency value of the inhibitor (IEtheor.%) from the largest to the smallest is MN2B2 > MNP3 > MN2P2 > MN3B > MP4 > MN3P > MNB3 > MN4 > MB4. Based on this data, it can be predicted that compounds with the addition of 2 boron atoms will have higher anti-corrosion efficiency (IE%) than other compounds, such as the addition of 4 boron atoms and 3 boron atoms. The addition of 4 boron atoms has the lowest inhibition efficiency value. Methenamine has an anti-corrosion efficiency (IE%) of mild steel of 70.21%, which is the anti-corrosion efficiency of carbon steel experimental results using the Tafel and EIS methods. The addition of 2 boron atoms has a good effect as a corrosion inhibitor, while 4 boron atoms have a less good effect as an inhibitor compared to other compounds. The efficiency of the inhibitor is affected by the ionization potential (IP) and electron transfer (ΔN). Theoretically, the smaller the ionization potential (IP), the greater the inhibitor efficiency value (IEtheor%). On the other hand, the

efficiency of the inhibitor (IE_{theor}%) is directly proportional to the electron transfer (ΔN). Figure 3 shows a visualization of methenamine's HOMO-LUMO-orbital and electrostatic potentials and its derivatives.

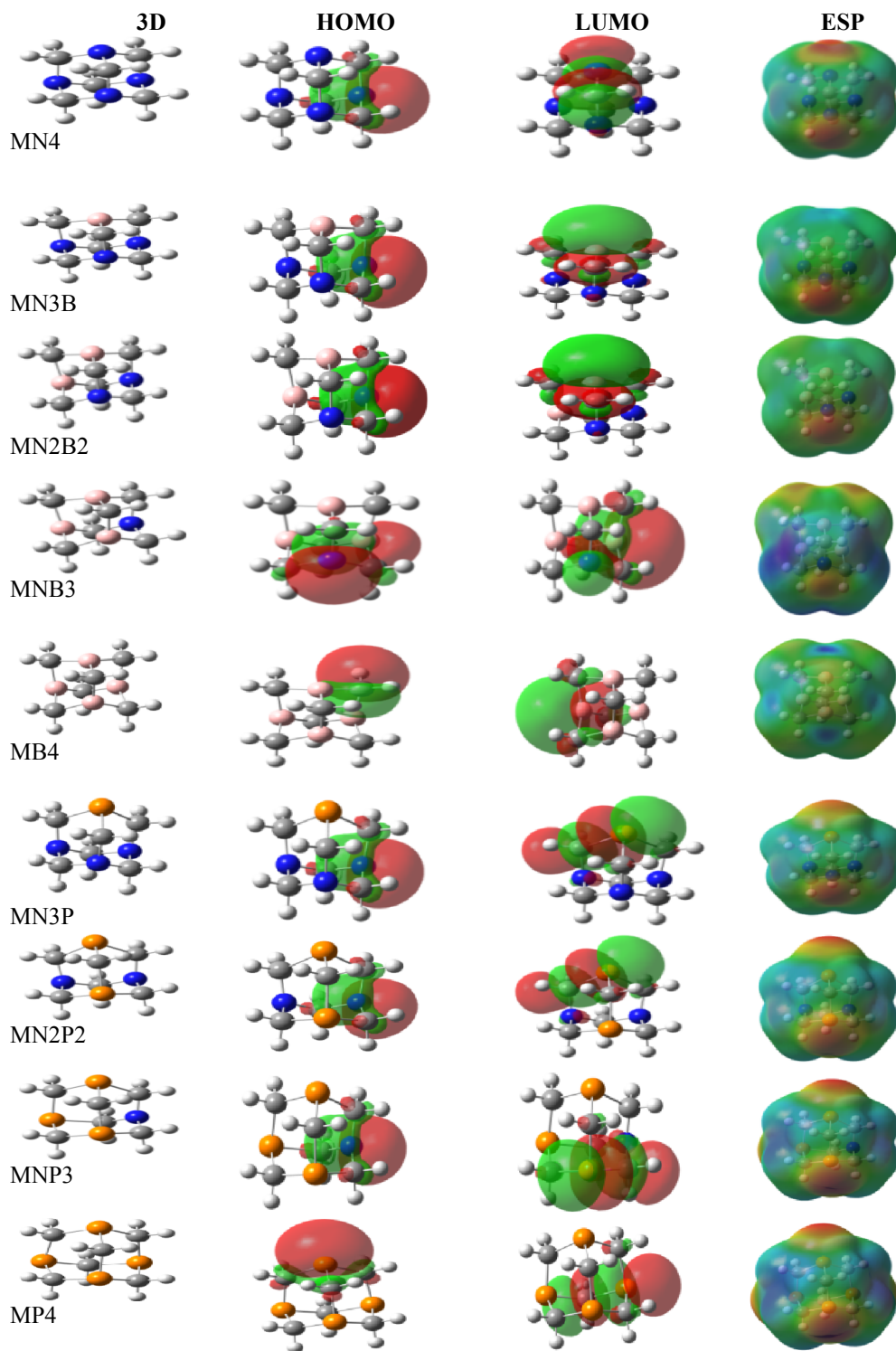


FIGURE 3. Visualization of HOMO, LUMO, and electrostatic potential

Table 3 shows that adding 4 boron atoms that do not involve nitrogen is a stable complex because it has good interaction with metals. The order of stability of the complex derivatives of cinnamic compounds is MB4 > MNB3 > MN2B2 > MP4 > MNP3 > MN2P2 > MN3P > MN4 > MN3B. It indicates that the compound with the addition of 4 boron atoms is a less good corrosion inhibitor (IE%) compared to other compound derivatives. Complex compounds are formed from the interaction of the central atom as a Lewis acid and ligands as a Lewis base or interactions based on the HSAB (Hard and soft acid and base) theory. Methenamine and its Fe conjugated derivatives are complex compounds, where bonds are formed between iron (Fe) with nitrogen (N) and other atoms such as boron (B) and phosphorus (P). This affects the bond length and bond angle of the compound. Meanwhile, the C atom acts as a ligand for the complex compound, the Nitrogen (N) atom as the base source. The HSAB theory is closely related to explaining covalent bonds and coordinating covalent bonds. Compared to nitrogen atoms, oxygen atoms have a higher tendency to form complex compounds with magnesium and iron metals. The tendency of the bond formed is an ionic bond and covalent coordination. The vacant orbital causes the coordination covalent bond on the Fe atom. The electron pair owned by the nitrogen atom will be coordinated/occupy the empty orbital to form a coordinate covalent bond. The complex of Fe-methenamine, boron, and phosphorus, Fe is a metal atom that uses empty s and d orbitals as acceptors to accept electron pairs from Nitrogen atoms. This visualization helps explain why the addition of 2 Boron atoms decreases while the addition of 4 Boron atoms has low reactivity.

Figure 3 shows that the addition of N, P heteroatoms, and other B atoms shows reactivity marked by red and green colors on each atom. The addition of 4 B atoms does not show reactivity because there is no red color between the atoms. Therefore, it can be predicted that the addition of 4 B atoms has poor anti-corrosion properties. In contrast, the addition of N, P heteroatoms, and another B atom shows that it is efficient as a corrosion inhibitor. Electron density is the area/space where electrons can be found. Electrons are an essential element in explaining the properties of molecules. We can predict the molecular structure, bond strength, reactivity, and stability with electrons. Electron density is often associated with the ESP surface, namely the probability of finding electrons at the Cartesian coordinates (x, y, and z) in a molecule. Table 4 shows that the nucleophilic differences are centered on the N atom (base donor strength 7.27). The electron charge distribution is more in the addition of N, P heteroatoms, and other B atoms. It is indicated by the number of yellow and red colors. The addition of 4 B atoms gives a lot of green colors. It means that methenamine is nucleophilic, and the addition of the B atom is electrophilic.

TABLE 4. Fukui using the DFT/6-311++G(d,p) method

Inhibitor	Atom	Fukui				
		N (-1)	N (0)	N(+1)	f(-)	f(+)
MN4	N10	0.39532	0.193141	0.25490	0.20218	0.06176
	N11	0.39557	0.192874	0.34833	0.20270	0.15546
	N12	0.39487	0.193617	0.25519	0.20125	0.06157
	C13	0.09740	0.128419	0.00829	0.03101	0.12012
	C16	0.09917	0.128726	0.02901	0.02954	0.09971
	N20	0.39565	0.193159	0.25477	0.20249	0.06161
MN2B2	N10	0.08234	0.000329	0.00485	0.08201	0.00518
	N11	0.07271	0.009712	0.01311	0.08242	0.00340
	B20	0.12574	0.051946	0.86920	0.07380	0.81726
	B22	0.12568	0.051866	0.86833	0.07381	0.81646
MB4	B10	0.35355	0.053008	0.06427	0.30054	0.01126
	B11	0.35127	0.052969	0.06348	0.29830	0.01051
	B12	0.35142	0.053002	0.06440	0.29842	0.01140
	B21	0.35100	0.054784	0.06497	0.29622	0.01019

The Fukui function can be used to determine the active site of a molecule in interacting with metal surfaces to prevent corrosion [52-54]. Table 4 shows the Fukui functions for methamine's nucleophilic and electrophilic attacks and its derivatives. It indicates that the C(13) and C(16) atoms act as electrophilic because they have high f+ values. Furthermore, N nitrogen atoms such as N(10), N(11), N(12), and N(20) act as nucleophilic attacks or donate

electrons to the metal surface. Adding boron and nitrogen, boron atoms act as electrophilic or accept electrons like B20 and B22 because they have a high f^+ . Therefore, the N atom acts as a nucleophile because it has a high f^- . With the addition of 4 boron atoms (MB4) which does not involve nitrogen, carbon acts as electrophilic and boron atom acts as nucleophilic characterized by high f^- value. The addition of a phosphorus heteroatom involving nitrogen. Carbon acts as electrophilic because it has a high f^+ value. Nitrogen and phosphorus have high f^- values, so they act as nucleophiles. With the addition of 4 phosphorus atoms that do not involve a nitrogen atom, carbon acts as electrophilic or accepts electrons characterized by a high f^+ value. In contrast, phosphorus acts as nucleophilic or donating electrons which are indicated by a high f^- value. The more negative a molecule is, the more electrons it will donate to other atoms. On the other hand, the more positive a molecule is, the more electrons it lacks

Natural Bond Orbitals show how much strength the interaction between atoms is. The NBO value involves the number of electron transfers expressed in energy. It affects the stability of the molecule [19,55]. Table 5 shows the second-order interactions clearly showing that the single electron pair (LP) of nitrogen and its derivatives and the single electron pair antibody (LP*) of Fe are responsible for the obtained E2 values. Donor interactions between Fe and MN4, MN3P, MN2P2, MNP3, MP4, MN3B, MN2B2, MNB3, and MB4 were 1.88, 1.79, 1.15, 1.14, 0.86, 1.76, 6.01, 4.90, 3.73 kcal.mol⁻¹, respectively. Based on these data, it can be seen that the addition of 2 Boron atoms has the highest E2 value of 6.01 kcal.mol⁻¹, which means that the addition of 2 Boron atoms and involves 2 N atoms have a high inhibitory efficiency (IE%), so it is good as a corrosion inhibitor. In comparison, the addition of 4 Boron atoms has a lower E2 value than other atoms. In addition to donating electrons, the nitrogen atom also reaccepts electrons donated by iron, even though the E2 value is low.

TABLE 5. Natural Bond Orbital (NBO) second interaction (E2) of methenamine compounds and their derivatives using the DFT/6-311++G (d,p) method

Gas			Solvent		
	Donor → Acceptor	E2 (kcal.mol ⁻¹)	Donor → Acceptor	E2 (kcal.mol ⁻¹)	
MN4	LP(4)Fe20-RY*(9)N21	1.88	LP(4)Fe20-RY*(9)N21	2.77	
	LP(4)Fe20-RY*(9)C13	0.55	LP(4)Fe20-RY*(9)C13	0.79	
	LP(4)Fe20-RY*(9)C16	0.57	LP(4)Fe20-RY*(9)C16	0.57	
MN2B2	LP(3)Fe20-RY*(3)B21	6.01	LP(3)Fe20-RY*(3)B21	3.24	
	LP(1)N19-BD*(1)Fe20	0.89	LP(1)N19-BD*(1)Fe20	0.78	
	LP(3)Fe20-RY*(1)C13	1.03	LP(2)Fe20-BD*(1)C13	1.48	
	LP(3)Fe20-RY*(2)C16	2.86	LP(3)Fe20-RY*(2)C16	1.83	
MB4	LP(3)Fe19-RY*(4)B20	3.73	LP(3)Fe19-RY*(4)B20	3.64	
	LP(3)Fe19-RY*(5)C13	0.55	LP(3)Fe19-RY*(5)C13	0.68	
	LP(3)Fe19-RY*(9)C16	1.11	LP(3)Fe19-RY*(9)C16	1.34	

CONCLUSION

Theoretical studies on the effect of heteroatoms on the efficiency of methanamine inhibition against carbon steels have been carried out. The results of the theoretical study show that the data are linear with the experimental study. The addition of 2 Boron atoms (MN2B2) has the highest inhibition efficiency. The lowest inhibition efficiency value was the addition of 4 boron atoms in the solution phase of 58.80%, so the addition of 4 boron atoms had poor corrosion inhibition. The results of this theoretical study can be taken into consideration in synthesizing new environmentally-friendly corrosion inhibitors.

REFERENCES

1. L. Jiang, Y. Dong, Y. Yuan, X. Zhou, Y. Liu, and X. Meng, *Chem. Eng. Sci.*, **430**, 132823 (2022).
2. L. T. Popoola, *Corros. Rev.* **37**, 2, 71-102 (2019).
3. A. Miralrio, A. Espinoza Vázquez, *Processes*, **8**, 8, 942 (2020).
4. A. A. Nazeer, and M. Madkour, *J. Mol. Liq.* **253**, 11-22 (2018).
5. C. Verma, D. K. Verma, E. E. Ebenso, and M. A. Quraishi, *Heteroatom. Chem.* **29**, 4, e21437 (2018).
6. Y. Ye, D. Zhang, Y. Zou, H. Zhao, and H. Chen, *J. Clean. Prod.*, **264**, 121682 (2020).

7. S. Hamdiani, I. H. Rohimah, N. Nuryono, A. A. Purwoko, L. R. T. Savalas, and S. Hadisaputra, *Asian J. Chem*, **31**, 303-308 (2019).
8. L. Feng, S. Zhang, Y. Qiang, Y. Xu, L. Guo, L. H. Madkour, and S. Chen, *Materials*, **11**, 6, 1042 (2018).
9. L. Gao, S. Peng, X. Huang, and Z. Gong, *Appl. Surf. Sci.*, **511**, 145446 (2020).
10. Z. Chen, A. A. Fadhil, T. Chen, A. A. Khadom, C. Fu, and N. A. Fadhil, *J. Mol. Liq*, **332**, 115852 (2021).
11. E. B. Caldona, M. Zhang, G. Liang, T. K. Hollis, C. E. Webster, D. W. Smith Jr, and D. O. Wipf, *J. Electro. Chem*, **880**, 114858 (2021).
12. S. Hadisaputra, A. A. Purwoko, I. Ilhamsyah, S. Hamdiani, and D. Suhendra, *Int. J. Corros. Scale Inhib*, **7**, 4, 633-647 (2017).
13. T. Laabaissi, M., Rbaa, F., Benhiba, Z., Rouifi, U. P., Kumar, F., Bentiss, F., and A. Zarrouk, *Colloids Surf. A Physicochem. Eng*, **629**, 127428 (2021).
14. H. Kumar, V. Yadav, S. K. Saha, and N. Kang, *J. Mol. Liq*, **338**, 116634 (2021).
15. H. Kumar, T. and Dhanda, *Chemical Data Collections*, **33**, 100721 (2021).
16. S. Hadisaputra, A. A. Purwoko, R. Rahmawati, D. Asnawati, I. Ilhamsyah, S. Hamdiani, and N. Nuryono, *Int. J. Electrochem. Sci*, **14**, 11110-11121 (2019).
17. Y. Boughoues, M. Benamira, L. Messaadia, and N. Ribouh, *Colloids Surf. A Physicochem. Eng*, **593**, 124610 (2020).
18. A. Kouache, A. Khelifa, H. Boutoumi, S. Moulay, A. Feghoul, B. Idir, and S. Aoudj, *J. Adhes Sci Technol*, **1**-29 (2021).
19. S. Hadisaputra, A. A. Purwoko, and S. Hamdiani, *Int. J. Corros. Scale Inhib*, **10**, 1, 419-440 (2021).
20. Y. Qiang, L. Guo, H. Li, and X. Lan, *Chem. Eng. Sci*, **406**, 126863 100354 (2021).
21. M. Yadav, T. K. Sarkar, and T. Purkait, *J. Mol. Liq.*, **212**, 731-738 (2015).
22. D. Wang, Y. Li, T. Chang, and A. Luo, *Colloids Surf. A Physicochem. Eng*, **628**, 127308 (2021).
23. S. Hadisaputra, A. A. Purwoko, A. Hakim, R. Wati, D. Asnawati, and Y. P. Prananto, (2020) "Experimental and Theoretical Study of Pinostrobin as Copper Corrosion Inhibitor at 1 M H₂SO₄ Medium" In *IOP Conference Series: Materials Science and Engineering* (Vol. 833, No. 1, p. 012010). IOP Publishing.
24. J. Haque, C. Verma, V. Srivastava, and W. W. Nik, *Sustain. Chem. Pharm*, **19** (2021).
25. R. S. Nathiya, S. Perumal, M. Moorthy, V. Murugesan, R. Rangappan, and V. Raj, *J. Bio- Tribo-Corros*, **6**, 1, 1-15 (2020).
26. A. Wahyuningsih, Y. Sunarya, and S. Aisyah, *J. Sains. Tek. Kim*, **1**, 1, 17-29 (2010).
27. A. Frisch, Gaussian 09W Reference. *Wallingford, USA*, 25p (2009).
28. T. Koopmans, *Physica*, **1**, 1, 6, 104-113 (1934).
29. A. Musa, A. B. Mohamad, A. A. Kadhum, M. S. Takriff, and W. Ahmoda, *J Ind Eng Chem*, **18**, 1, 551-555 (2012).
30. N. Islam, and D. Chandra Ghosh *Mol. Phys*, **109**, 917-931 (2011).
31. R. G. Parr, L. V. Szentpaly, and S. Liu, *Electrophilicity index. J. Am. Chem. Soc.* **121**, 9, 1922-1924 (1999).
32. W. Yang, and R. G. Parr, *Proc. Natl. Acad. Sci*, **82**, 6723-6726 (1985).
33. R. G. Pearson, *Coord. Chem. Rev*, **100**, 403-425 (1990).
34. R. G. Pearson, *Inorg. Chem*, **27**, 734-740 (1988).
35. H. R. Obayes, G. H. Alwan, A. H. M. J. Alobaidy, A. A. AlAmiery, A. A. H. Kadhum, and A. B. Mohamad, *Chem. Cent. J.*, **8**, 21 (2014).
36. S. Hadisaputra, S. Hamdiani, M. A. Kurniawan, and N. Nuryono, N. (2017). *Indones. J. Chem*, **17**, 3, 431-438 (1988).
37. S. Hadisaputra, L. R. Canaval, H. D. Pranowo, and R. Armunanto, *Monats. Chem*, **145**, 5, 737-745 (2014).
38. K. Karakus, and K. Sayin, *J. Taiwan Inst. Chem. Eng*, **48**, 95-102 (2015).
39. I. B. Obot, and Z. M. Gasem, *Corros. Sci*, **83**, 359-366, (2014).
40. G. Singh, B. P. Baranwal, I. P. S. Kapoor, and D. Kumar, *J. Phys. Chem. A*, **111**, 12972-12976 (2007).
41. S. Hadisaputra, Z. Iskandar, and D. Asnawati, *Acta Chim. Asiana*, **2**, 1, 88-94 (2019).
42. B. Tüzün, and J. Bhawsar, *Arab. J. Chem*, **14**, 2, 102927 (2021).
43. S. Hadisaputra, A. A. Purwoko, L. R. T. Savalas, and N. Prasetyo, E. Yuanita, S. Hamdiani, *Coatings*, **10**, 11, 1086 (2020).
44. N. B. Iroha, N. A. Madueke, V. Mkpenie, B. T. Ogunyemi, L. A. Nnanna, S. Singh, and E. E. Ebenso, *J. Mol. Struct.*, **1227**, 129533 (2021).
45. F. Wajdi, S. Hadisaputra, and I. Sumarlan, *Acta Chimica Asiana*, **1**, 2, 43-49 (2018).

46. I. A. Alkadir Aziz, I. A. Annon, M. H. Abdulkareem, M. M. Hanoon, M. H. Alkaabi, L. M. Shaker, and M. S. Takriff, *Lubricants*, **9**, 12, 122 (2021).
47. A. Hadisaputra, A. A. Purwoko, A. Hakim, L. R. T. Savalas, R. Rahmawati, S. Hamdiani, and N. Nuryono, "Which anthocyanin is the best corrosion inhibitor?" In *Journal of Physics: Conference Series* (). (IOP Publishing, 2019), Vol. 1402, No. 5, p. 055046.
48. A. A. Khadom, S. A. Jassim, M. M. Kadhim, and N. B. Ali, *J. Mol. Liq.* 117984 (2021).
49. S. Hadisaputra, A. A. Purwoko, Y. Wirayani, M. Ulfa, and S. Hamdiani, "Density functional and perturbation calculation on the corrosion inhibition performance of benzylnicotine and its derivatives." In *AIP Conference Proceedings* (AIP Publishing LLC, 2019), Vol. 2243, No. 1, p. 020006.
50. S. Hadisaputra, A. A. Purwoko, S. Hamdiani, and N. Nuryono, "Ab initio MP2 and DFT studies of ethyl-p-methoxycinnamate and its derivatives as corrosion inhibitors of iron in acidic medium." In *IOP Conference Series: Materials Science and Engineering* (IOP Publishing, 2019), Vol. 509, No. 1, p. 012129.
51. S. Hamdiani, I. H. Rohimah, N. Nuryono, A. A. Purwoko, L. R. T. Savalas, S. Hadisaputra, *Asian J. Chem*, **31**, 303-308 (2019).
52. A. T. Rani, A. Thomas, L. Williams, A. Joseph, *J. Bio- Tribo-Corros*, **8**, 1, 1-21 (2022).
53. P. Xu, J. Zhou, G. Li, P. Wang, P. Wang, F. Li, H. Chi, *Constr Build Mater*, **288**, 123101 (2021).
54. M. A. Mostafa, A. M. Ashmawy, M. A. A. Reheim, M. A. Bedair, A. M. Abuelela, *J. Mol. Struct*, **1236**, 130292 (2021).
55. B.D. Mert, A.O. Yüce, G. Kardaş and B. Yazıcı, *Corros. Sci.*, **85**, 287–295 (2014).